PCCP

Fluorescent carbon nanomaterials: "quantum dots" or nanoclusters?

Journal:	*Physical Chemistry Chemical Physics*
Manuscript ID:	CP-ART-01-2014-000138.R3
Article Type:	Paper
Date Submitted by the Author:	02-Jun-2014

Complete List of Authors:	Dekaliuk, Mariia; Palladin Institute of Biochemistry, Laboratory of Nanobiotechnology Viagin, Oleg; Institute for Scintillation Materials, Malyukin, Yuri; Institute for Scintillation Materials, Demchenko, Alexander P.; Palladin Institute of Biochemistry, Laboratory of Nanobiotechnology

Fluorescent carbon nanomaterials: "quantum dots" or nanoclusters?

Mariia O. Dekaliuk[a], Oleg Viagin[b], Yuriy V. Malyukin[b], Alexander P. Demchenko[a]

[a]*Laboratory of Nanobiotechnology, Palladin Institute of Biochemistry, Leontovicha st. 9, Kyiv 01030, Ukraine*

[b]*Institute for Scintillation Materials, STC "Institute for Single Crystals", 60 Lenin Ave., 61001 Kharkiv, Ukraine*

Despite many efforts, the mechanisms of light absorption and emission of small fluorescent carbon nanoparticles (C-dots) are still unresolved and is a subject of active discussion. In this work we address the question if the fluorescence is a collective property of these nanoparticles or they are composed of assembled individual emitters. Selecting three types of C-dots with "violet", "blue" and "green" emissions and performing detailed study of fluorescence intensity, lifetime and time-resolved anisotropy as a function of excitation and emission wavelengths together with the effect of viscogen and dynamic fluorescence quencher, we demonstrate that the C-dots represent the assemblies of surface exposed fluorophores. They behave as individual emitters, display electronic anisotropy, do not exchange their excited-state energies via homo-FRET and possibly display the sub-nanosecond intra-particle mobility.

1. Introduction

Unusual optical properties of carbon nanomaterials have attracted the attention of many researchers.[1-4] The attempts to explain them based on analogy with well studied fluorophores, such as organic dyes[5] or semiconductor nanoparticles[6] did not bring consensus in their description. Fluorescent carbon nanoparticles are broadly variable structures that include short fragments of graphene, graphene oxide and nanotubes and also the 'carbon dots' (C-dots). The latter are diverse in production, composition and chemical modification of their surface.[1, 3, 7-9] They are attractive for many applications substituting traditional luminophores owing to their simple and cheap synthesis and stability in aqueous medium, high photostability, the absence of toxicity and multiple possibilities for their chemical modifications. The progress in understanding of their photophysical properties must stimulate a variety of new applications allowing their modification and adaptation to particular tasks.

Therefore in the present research we decided to address the simple but yet unresolved questions. Is the fluorescence response generated by the whole nanoparticle displaying collective excitonic effect, such as in semiconductor quantum dots,[10] or it represents the superposition of responses of assembled individual emitters, such as in dye-doped polymers?[11] If there are individual emitters, do they emit individually or they exchange the excitation energies, so that a

generated collective effect is in origin of their emission? Specifically, we have to select between three models depicted in Fig. 1.

In the first case of "collective" emission, the nanoparticle should respond as a whole, and, since the exciton confinement effects confer size-dependence, the spectral heterogeneity may appear due to the distribution of particle sizes with some influence of variation in composition of surface-modifying groups. Then the parameters of fluorescence emission should be insensitive or low sensitive to solvent perturbations. The particles should behave similarly displaying no heterogeneity with respect to dynamic quenching by heavy atoms dissolved in the solvent. Fluorescence emission should not be polarized, and if present due to structural asymmetry (such as in "quantum rods" [12]), the whole-particle rotational diffusion depolarizing the emission should be much slower than the emission decay rate.

Quite different effects are expected in the case of "individual" emissions of multiple fluorophores assembled in each nanoparticle. The expected variation in their structures and interactions should result in heterogeneity of their optical properties, leading to detectable wavelength-resolved spectroscopic effects.[13, 14] Their excitation with polarized light may generate optical anisotropy.[15, 16] If the nanosecond mobility of these emitters is present within the nanoparticle, it should be revealed in time-resolved anisotropy. Such mobility is expected to be suppressed in highly viscous media leading to significant effects in anisotropy decay rates.

The third possibility, the "light harvesting" emission can be considered as an intermediate between the two limiting cased discussed above but with its own characteristic features. Being confined in the nanoparticle structure, the individual emitters may be located at short distances that are sufficient for the exchange of their excitation energies via the well-known FRET mechanism.[17] In the case of multiple emitters with spectral heterogeneity the FRET effects, even if the emitters are the same (homo-FRET) but their environments differ, are quite characteristic. The energy harvested by emitters absorbing the light quanta at the short wavelength side of the spectrum is transferred to those emitters (acceptors) that absorb and emit light of the lowest energies, at longest wavelengths. This should reduce the emission heterogeneity and lead to very specific effects in anisotropy. The FRET should lead to depolarization of emission that should be time-dependent and wavelength-dependent [18]. At short emission wavelengths the polarized emission of the donors can be seen, and since FRET results in depolarization, at long wavelengths the depolarized emission of the acceptors should be predominant. The shift of excitation to the long wavelength edge instead of exciting the donors selects the polarized emission of the acceptors (the Red Edge effect[14, 19]). These effects, if they exist in solid environment within the nanoparticle, should not depend on solvent viscosity.

Thus, in the present report we make an attempt to resolve the questions addressed to the origin of C-dots emission by studying the wavelength-resolved effects in the excitation and emission spectra, the emission decays and time-resolved anisotropy over these spectra and also the effects of solvent perturbant and viscogen on these parameters. Additionally, we apply the quenching by heavy atom with an attempt to resolve the response from surface and interiorly located emitters. In order to probe the generality of observed regularities we synthesized three

types of C-dots from different starting materials that differ dramatically in their quantum yields and positions of fluorescence spectra and use them in the present study.

2. Materials and methods

The C-dots were prepared from alanine, glycerol and sucrose dissolved in aqueous media. The most effective and easy methods for obtaining the carbon dots that are based on microwave (MW) treatment were applied. By these methods the nanoscale materials have been obtained with different optical characteristics, denoted as "violet", "blue" and "green" C-dots. These carbon nanostructures were prepared by the methods used in other works with only small modifications, specifically:

"Violet" C-dots were prepared from β-alanine by the method of Jiang[20] that was primarily applied for the microwave treatment of histidine. Specifically: 0.5 g of β-alanine was dissolved in 2 ml of distilled water in open vessel and treated in microwave oven (600 W, 1.5 min). The obtained material was diluted with distilled water and followed by repeated centrifugation (10 min×5000 g) with the collection of supernatant. To obtain an accurate concentration of the particles, the supernatant was dried to the attainment of constant weight. Thereafter, 7 mg/ml concentration was prepared by dissolving the product in distilled water to conduct further research.

"Blue" C-dots were obtained by microwave treatment of glycerol solution[21]. Specifically: 5 ml of glycerol was mixed with 3 ml of Ringer's solution (pH 7.4) and 2 ml of distilled water and then treated in MW oven at 700 W for 6 minutes. The resulting product was diluted with distilled water.

"Green" C-dots were obtained from the mixture of sucrose and polyethylene glycol (PEG) in aqueous solution[22]. Specifically: 4g sucrose was mixed with 0.5 g PEG-150 and diluted in 26 ml distilled water. After that the sample was treated in MW oven (600 W, 4 min), and 30 ml water was added, diluting the sample. These particles tend to associate with the change (long-wavelength shift) of fluorescence spectra, so in some experiments additional ultrasonic treatment was used.

Steady-state light absorption and fluorescence spectra were recorded on spectrophotometer Lambda Bio (Perkin Elmer) and spectrofluorimeter QuantaMaster (Photon Technology International) accordingly. Quantum yield of fluorescence was determined by the common reference-based method using quinine sulfate as the standard.[23] The low absorbance of the samples and the absence of well-resolved maxima at the wavelength of excitation induce some uncertainty in these determinations. Fluorescence quenching by iodide ion and determination of fluorescence quenching constants from Stern-Volmer plots were performed as described.[24]

Time-resolved fluorescence measurements and data analysis were performed using FluoTime200 picosecond spectrofluorimeter and FluoFit software respectively (PicoQuant). The laser heads with the emission wavelengths at 330 nm and 380 nm were used as the excitation

sources.

Nanoparticle size was determined using a ZetaPALS/BI-MAS analyzer (Brookhaven Instruments Corp., USA) operated in phase analysis light scattering mode. Measurements were carried out at the scattering angle at 90° and laser illumination at 659 nm. The temperature of experiments was 25°C.

3. Results

3.1. Spectroscopic characterization

The C-dots studied in this work display both common and specific spectroscopic properties. Common is the very strong absorbance in the UV range and the absence of comparable level of absorbance at the wavelengths of maxima of excitation spectra (Fig. 2). All the species exhibit the absence of fluorescence emission excited at the maximum of UV excitation band. Such behavior is quite different from that of semiconductor quantum dots but is common for carbon dots[25, 26] and also for graphene and graphene oxide nanoparticles.[1, 4] It was explained by the presence of two types of chromophores, non-emitting and those emitting in the visible range that are related to different elements of their structures.[1, 3]

There is a common agreement on the general principles of formation of C-dots from organic matter in aqueous media. The core is formed by inorganic carbon in the form of sp^2 hybridized two-dimensional graphene-type islands[27] disrupted by sp^3 hybridized diamond-type inclusions.[28, 29] Polar groups derived from starting materials in the formation of nanoparticles become exposed to the surface that allows the particles to be soluble in water. Remarkable similarity in Raman spectra of particles obtained from different starting materials demonstrating the presence of sp^2 and sp^3 hybridized structures in similar proportions[29, 30] suggests similarities of their properties. It is known that in aggregates of π-electronic heterocyclic structures the fluorescence is strongly quenched[31] and graphene and other carbon materials are strong quenchers of fluorescence of aromatic molecules by the mechanism of excited-state electron transfer.[32, 33] It was also observed that in multiple-layer graphene sheets the fluorescence is dramatically quenched in comparison with single-layer sheets.[34] These effects explain the strong UV absorption and the absence of emission in all three types of studied here nanoparticles. Collective excitations, when they propagate over percolated π-electronic islands, lead to quenching, so we have a family of light absorbers but not emitters.

In contrast, the fluorescence properties of C-dots are attributed to particle shells.[35-37] Here the starting material forming the composition of polar groups on the particle surface is of ultimate importance. The Fig.3 presented below outlines the similarities and differences in their structures.

Thus, all studied water soluble C-dots obtained by thermal treatment of organic materials contain oxygen in the form of hydroxyls, carboxyls and carbonyls.[38] Using amino acids as the starting material results in inclusion into the polar shell the nitrogen-containing groups in the

form of primary amines and aromatic pyroles. This inclusion is known to increase the quantum yield of fluorescence and to shift the fluorescence spectrum to shorter wavelengths.[39, 40] Our spectroscopic data for "violet" C-dots are in line with these results. The excitation band is located at 350 nm with the shoulder at 315 nm. Only a small shift in emission spectrum is observed with variation between these excitation wavelengths. The fluorescence quantum yield is high, 28%, which is an indicator of their high brightness (Table 1).

The "blue" C-dots were obtained by thermal treatment of glycerol-water mixture in the presence of Na^+, K^+ and Ca^{++} cations (Ringer's solution). These ions are included into polar shells of formed particles, which allows increasing dramatically their quantum yield.[21] In this case also, no absorption band is detected at the position of excitation band at 350 nm. The excitation band possesses the short wavelength shoulder, which is presented as a small intensity feature in the absorption spectra. The quantum yield is lower, 5.4 %.

The "green" C-dots were obtained from organic predecessors that contained beside carbon only oxygen. Their excitation band maximum that is shifted to longer wavelengths (to 425 nm) and at this wavelength the absorbance is very low. Fluorescence emission band maximum is located at 530 nm. The quantum yield is much lower (2.1%).

Due to the absence of collective effects in emission, in carbonic nanoparticles there is no strong correlation between the position of spectra and particle size,[41] which is contrary to semiconductor quantum dots.[10] Therefore we connect the spectral differences with different composition of the particle surfaces. All three types of nanomaterials exhibit the wavelength-dependent heterogeneity of fluorescence emission, so that the excitation spectra shift as a function of emission wavelength, and the emission spectra shift as a function of excitation wavelength. Though less significant than those reported in the literature, [1, 3, 4] they demonstrate certain extent of structural heterogeneity. Meantime, it is not clear from these data, if the source of such heterogeneity is the distribution of optical properties between the nanoparticles, each of them demonstrating collective response or between the individual emitters within these nanoparticles.

Thus, all three types of nanoparticles regarding their visible fluorescence behave like organic dyes, demonstrating discrete excitation bands that (almost) mirror image the emission spectra. The absorption bands do not show their maxima at the positions of excitation bands being hidden under the tails of much stronger absorption in the UV. The graphite-like structures of which the C-dots are composed are known as strong quenchers of fluorescence of organic dyes[33] and it is not clear why this does not happen in the present case with the emission in the visible range. Probably the static disorder of the surface exposed cites prohibits the steric arrangements that could be favorable for electron-transfer quenching.

3.2. Fluorescence quenching by external quencher

The fluorescence quenching by ionic quencher dissolved in the solvent is a simple and convenient tool to characterize the surface exposure of fluorophores and heterogeneity in this

exposure. This method is commonly used in the studies of proteins in aqueous solutions.[24] The quenching by heavy atom (the Kasha effect) requires direct contact between fluorophore and the quencher so that the fluorophores hidden from the quencher in the particle core have to continue emitting normally. In our work we used the quenching by iodide anion, which is known as one of the most potent ionic quenchers.[24] We took into account that since the particle surface is negatively charged, the static interaction with quencher anion will not be efficient and the quenching of surface exposed emitters will occur in collisional manner.

Our results presented in the form of Stern-Volmer plots demonstrate the high availability of fluorophores to quenching, of the order 10^9-10^{10} M^{-1} s^{-1} (Table 1). Such high values of quenching constants may suggest the involvement of not only dynamic but also static heavy atom quenching effects. If it exists it should also operate on direct contact with the fluorophore. In addition, linearity in Stern-Volmer plots (Fig. 4 and Figs. S1-S2, Supporting Information) indicates the absence of heterogeneity in fluorophore exposure strongly suggesting the absence of intrinsically located emitters that are not available for quenching.

The spectral shifts on the action of quencher are undetected, which is the support for the absence on quenching of selectivity between the emitters that could possess spectral differences. The structural heterogeneity giving rise to wavelength-selective effects should originate within the surface-exposed species only. Therefore the suggestions on the origin of spectral heterogeneity as the interplay of emission from the core and surface states[36, 42] are not supported in the present experiments.

Summarizing this series of experiments we conclude that the studied fluorescent C-dots synthesized from different sources, differing in wavelengths and quantum yields of their emission, display quite similar properties regarding spectral heterogeneity and availability to quenching.

3.3. Fluorescence emission decays

The fluorescence decay in a system of identical fluorophores if they interact similarly with their environment and do not display the excited state reactions is strictly single-exponential.[43] Non-exponentiality may appear due to several reasons: the presence of two or multiple emitting ground-state forms, excited-state reactions, etc. The results for “violet” C-dots presented in Fig. 5 and for “blue” and “green” C-dots in Figs. S3-S4, Supporting Information, demonstrate that all their decay kinetics are similar in character and strongly non-exponential. The absence of appreciable excitation wavelength dependence of decay kinetics does not favor interpretation of these results in terms of discrete ground-state species (that should differ spectroscopically) and does not justify deconvolution of decay functions into two or more discrete lifetime components. If, in contrast, we assume continuous distribution of lifetimes around the most probable value, the most appropriate could be the approximation by stretched exponential function (Kohlrausch decay function):[43, 44]

$$I(t) = I_0 \exp\left[-(t/\tau)^{\beta}\right] \quad (1)$$

Here τ and β are the parameters describing stretched exponential decays, τ has the dimension of time and $0< \beta \leq 1$. Generally, a smaller value of β corresponds to a wider distribution of lifetimes, suggesting a more disordered system. In all the cases we observe quite satisfactory fit of fluorescence intensity decays to functions expressed by Eq. (1), see Table 2 and Figs. S3-S4, Supporting information, justified by random distribution of residuals (data not shown). The values of β about 0.5 observed in our experiments, are observed both in contact collisional quenching in solutions and in solids with low structural order.[44] Such behavior suggest the "distributed" character of decays from individual emitters, which is due to their continuous distribution possessing variation in decay rates.

It is known that the non-exponential behavior in emission decays appears also if the fluorophores exhibit any of the excited-state reactions, such as the charge transfer (CT) or FRET.[45] These reactions occur with the decrease of energy, which depopulates the emitters at short wavelengths and repopulates those absorbing and emitting at longer wavelengths. If these effects are present, they should vanish at the red edge excitation, since only the FRET acceptors or the CT states can be excited in this case and their fluorescence decay kinetics should be different from that excited at the band maximum or at its blue edge.[46] Thus, the observation of spectral dependences of decays provides a strong criterion for the occurrence or not occurrence of these reactions within the lifetime of fluorescence emission.

So, if we compare the decays obtained for the "violet" C-dots at different emission wavelengths obtained at the band maximum excitation 330 nm (Table 2) we observe that with the exception of decay at the far blue edge at 360 nm (the origin of which is unknown), the decays do not show any strong dependence on emission wavelength. Essentially, no such dependence is seen at the red edge of emission (500 nm) compared to the result at the band maximum (450 nm). This result is contrary to that expected in the case of FRET between the emitters, since such transfer of energy should occur in a direction from short-wavelength to long wavelength emitters increasing the lifetimes at long emission wavelengths. Therefore we do not observe any indications of the presence of FRET or other excited state process occurring with the decrease of excitation energy.[19] These data are quite consistent with the results obtained for "blue" and "green" C-dots (Figs. S3-S4, Supporting information).

If the applied excitation wavelength for "violet" dots is shifted to the red edge (380 nm) there are observed, similar (somewhat shorter) decays, compared to that at the main-band excitation. They are also almost emission wavelength independent (Table 2). In this way a photoselection is provided of those fluorophores that are excited and emitting at lower energies than the mean of their distribution, so that they are unable to participate in the excited-state

reactions.[19] We observe that their lifetimes are shorter and, as expected, they do not depend on emission wavelength. Similar experiments were performed with "blue" and "green" C-dots (see Supporting Information, Figs. S3-S4). They led to quite similar results.

Additional studies of fluorescence decays in water:diethylene glycol (1:1 v/v) solvent we performed in all three systems. Diethylene glycol is known as the viscogen and also as the perturbant decreasing the polarity of water and perturbing its hydrogen-bonded network. In our case we observe the well-reproducible decrease of fluorescence intensity demonstrating the interaction of fluorophores with the perturbant and supporting the view on their surface location.

In view of strong Stokes-shifted fluorescence emission observed in all our cases (as well in many literature data[1-4]), we have to consider the possibility of some type of relaxations shifting the spectra as a function of time. Relaxations have to shift the spectra to longer wavelengths, so in intensity decays we have to observe the shorter lifetimes at short emissions and longer lifetimes at long emissions. Also the long-wavelength excitation selects the "relaxed" states, so one may observe longer decays. These effects are not seen in our data, suggesting that these relaxations are intra-chromophoric and that they must occur at much shorter times than the temporal resolution of our experiment.

Taken together, these data witness for the absence of FRET effects or of any other excited-state reactions producing time-dependent spectral shifts in the sub-nanosecond-nanosecond time range. Providing the excitation and observing the emission at different wavelengths we could not detect the energy flow from short-wavelength excited donors to long-wavelength emitting acceptors, which indicates that all the fluorophores emit independently. The structural heterogeneity is revealed basically by the strongly non-exponential fluorescence emission decays.

When we compare the three types of C-dots (see Table 1), we note the absence of correspondence between quantum yields and lifetimes. Dramatic difference in quantum yields within the same range of lifetime values suggests that the emission of significant amount of fluorophores in the population of "blue" and, more significantly, "green" C-dots is statically quenched. Similar conclusion can be derived if the literature data are compared. The reported photoluminescence lifetimes of C-dot emission (up to ~6-8 ns [25, 47, 48]) do not depend strongly on sample source and preparation, but display manifold variation in quantum yields. This suggests the involvement of strong and selective static quenching effects leading to non-fluorescent nanoparticles. This issue is notable and should be resolved on a single particle level.

3.4. Fluorescence anisotropy and its decay function.

The measurements of emission anisotropy are very popular in the studies of polymers and biological macromolecules.[16] The linearly polarized light excites preferentially those molecules or particles whose transition dipole moment is parallel to the light field, leading to polarized emission. High initial anisotropy decreases with time due to the loss of initial orientation as a result of rotational diffusion or of the energy transfer to other emitters. The distinction between

these two depolarizing factors is crucial in the analysis of anisotropy decays of carbonic nanoparticles.

The anisotropy $r(t)$ describing the fluorescence depolarization with time is defined by the following relation:

$$r(t) = \frac{I \parallel (t) - I \perp (t)}{I \parallel (t) + 2I \perp (t)} \qquad (1)$$

where $I\parallel(t)$ and $I\perp(t)$ are the intensities of light polarized parallel and perpendicular to the direction of polarization the laser excitation. The simplest function describing anisotropy decay is single exponential:

$$r(t) = r_0 \exp(-t/\tau_r) \qquad (2)$$

Here r_0 is the initial value of the anisotropy. $r(t)$ can change between the theoretically achievable value $r_0 = 0.4$ and zero.

The time behavior of the anisotropy decay $r(t)$ is well described by a single exponent with a characteristic time, τ_r, (Eq. 2) only for the particle of spherical shape. The depolarizing rotational motions can be recognized by an independence of anisotropy decay on excitation or emission wavelength and by its strong dependence on solvent viscosity. In this case the analysis of fluorescence anisotropy reveals the characteristic rotational time of fluorophores and of the particles to which they are rigidly incorporated.

It is known that fluorescence anisotropy is absent for spherical nanoparticles exhibiting collective-type mode of fluorescence emission, e.g. semiconductor nanocrystals (quantum dots)[10] and if such anisotropy exists in "quantum rods"[12], its time-resolved decay in solutions is associated with rotation of the whole particles. Therefore the presence of highly polarized emission of these quasi-spherical particles (Fig. 5 and Figs. S5-S6, Supporting information) is surprising. In addition to structural anisotropy there should exist strong electronic polarization in the excited states that can allow photoselection by polarized light of fluorophores in particular orientation resulting in polarized emission.[43] It is not clear, how carbon nanoparticles can achieve these properties.

Our results demonstrate that in all studied systems there are fast anisotropy decays with the rates leading to τ_r values of the order of 0.5-0.7 ns (Table 3 and Figs. S5-S6, Supporting information). Based on these values and assuming spherical shape of the particle and its free rotation we can roughly estimate the size of rotating unit r_{hy} using the classical Stokes-Einstein equation, as it was done by others.[49]

$$r_{hy} = \left(\frac{3k_B T \tau_r}{4\pi\eta}\right)^{1/3}, \qquad (3)$$

where k_B is Boltzmann's constant, T the temperature (K), η is the viscosity and τ_r is the rotational relaxation time. We obtain the result of 0.7-0.8 nm. This estimated size does not correspond to actually determined particle size (see Table 1) and is much smaller. Such values do not conform to the notion that the studied nanoparticles are integral emitters with permanent excited-state dipole moments. For estimates,[50] the rotations of protein molecules of similar size are observed in the range 10^{-6}-10^{-7} s, whereas for small organic dyes with the size of 0.4-0.5 nm in low-viscous media at room temperature the rotational correlation times are between 0.1 and 0.2 ns.

The absence of such correspondence required performing additional experiments. We observed that for "violet" C-dots the rotational correlation time increases strongly with the addition of diethylene glycol (DEG) that can be considered as a strong viscogen (Fig. 6 and Table 3). With this addition the solvent viscosity increases from ~1 mPa×s (the viscosity of water at 20^0 C) to about 4.8 mPa×s. The fact of such strong τ_r increase witnesses for the retardation of rotational mobility in the system. Comparing these data with the results for "blue" and "green" particles (Figs. S5-S7, Supporting information) we observe a similar trend. We note that there is no correlation with the particle size (see Table 1), which, together with short τ_r values suggests the presence of intra-particle local depolarizing mobility.

Our results on strong influence on τ_r by the viscogen do not support the possibility of involvement of FRET as the origin of depolarization of emission. The other witness for inefficiency of FRET is given by the absence of strong dependence of anisotropy decays on excitation and emission wavelength. If the fluorophores within short distances between them (in our case incorporated into the same nanoparticle) exchange their excitation energies, this process known as homo-FRET should be observed. Its distinguishing features are the characteristic dependences of positions of spectra and of anisotropy decays on the excitation and emission wavelengths. Even if the fluorophores are structurally identical, their distribution must exist on interaction energy with the environment. Providing the excitation and observing the emission at different wavelengths one must detect the energy flow from short-wavelength excited donors to long-wavelength emitting acceptors causing depolarizing effect.[46] Such dependence should be strong and characteristic. At the main-band excitation at short wavelengths of emission the FRET donors can be selectively excited and emit the highly polarized light. With the shift to longer wavelengths we have to see the emission of acceptors, which should be highly depolarized.[51] The experiment does not show such feature (Fig. 5 and Figs. S6-S7, Supporting information).

The red-edge excitation at 380 nm (Table 4) allows providing additional criteria for the distinction between rotations and FRET as the mechanisms of time-resolved depolarization of

emission. Rotational depolarization does not depend on the wavelengths of excitation or emission, but should be sensitive to viscogen addition. On contrary, the red-edge excitation, selecting the FRET acceptors, should provide higher initial anisotropy and slower its decay rate.[46] Therefore the results showing strong viscosity dependence and only a small spectral dependence (Fig. 6 and Tables 3-4) are the strong arguments for the local intra-particle rotational dynamics and the absence of FRET. Notably, these results obtained for "violet" C-dots are in good agreement with that obtained for two other types of carbon nanoparticles (see Figs. S6-S7, Supporting information), suggesting that such behavior is quite general.

4. Conclusions and prospects.

At present time the physical origin of fluorescence emission from carbon nanoscale materials is unclear with numerous fundamental questions as yet unresolved. Therefore the versatile insights obtained from various experimental approaches are needed to clarify this interesting and important issue. In our work, detailed study of fluorescence spectra, quantum yields, steady-state quenching and also the lifetime and time-resolved anisotropy as a function of excitation and emission wavelengths was performed for three types of C-dots with "violet", "blue" and "green" emissions. They demonstrate the presence within the nanoparticles of distribution of individual emitters that do not exchange their excited-state energies via FRET mechanism. The studies of time-resolved anisotropy reveal the sub-nanosecond local intra-particle mobility of these fluorophores that is retarded in viscous medium, and the quenching experiments demonstrate their location at nanoparticle surface.

We demonstrate that contrary to views of many scientists,[34-352-55] the C-dots are not 'quantum dots' and even not the 'dots'. Because of the presence of electronic anisotropy they cannot be considered as 'dots', the objects of zero dimension. Moreover, their fluorescence response is not collective and represents composition of individual emitters. According to the present results, they are the nano-sized clusters assembling individual fluorophores. In line with the views of other scientists [35-37] these emitters are formed on the particle surface. The latter possess the following properties:

- They are exposed to the solvent and can be easily quenched by diffusional quencher.
- They display spectral distribution and distribution of emission decays in a rather limited range.
- They display anisotropy of fluorescence emission and sub-nanosecond anisotropy decay that suggests their limited rotation within the particle.
- They emit individually and do not exchange energies via FRET mechanism.

We believe that our methodology based on combination of spectroscopic, time-resolved and anisotropy studies will be useful in research on other fluorescent nanoscale materials. Of particular importance are graphene oxides, for which also a consensus regarding the emissive states has not been reached and debates between the followers of molecule-like surface-exposed

emissive states[5], the aromatic islands within the particle core[56] and these states formed by exciton propagation within the particle volume[6, 57] continue.

Due to simple and cheap synthesis and stability in aqueous medium, high photostability, the absence of toxicity and multiple possibilities for their chemical modifications, the carbon nanoparticles can be efficiently used in various fields of science and technology substituting traditional luminophores.[9, 58] They are very promising platforms for assembly of multifunctional nanocomposites for applications for *in vivo* diagnosis and drug delivery.[59-61] The understanding of their optical properties has to lead to the ability to modulate them for optimal performance.

References

1. L. Cao, M. J. Meziani, S. Sahu and Y. P. Sun, *Accounts of Chemical Research*, 2012, **46**, 171-180.
2. S. Chandra, P. Das, S. Bag, D. Laha and P. Pramanik, *Nanoscale*, 2011, **3**, 1533-1540.
3. A. P. Demchenko and M. O. Dekaliuk, *Methods Appl. Fluoresc.*, 2013 **1**, 042001 doi:042010.041088/042050-046120/042001/042004/042001.
4. L. Li, G. Wu, G. Yang, J. Peng, J. Zhao and J. J. Zhu, *Nanoscale*, 2013, **5**, 4015-4039.
5. C. Galande, A. D. Mohite, A. V. Naumov, W. Gao, L. Ci, A. Ajayan, H. Gao, A. Srivastava, R. B. Weisman and P. M. Ajayan, *Sci Rep*, 2011, **1**, 85 DOI: 10.1038/srep00085.
6. J. Shang, L. Ma, J. Li, W. Ai, T. Yu and G. G. Gurzadyan, *Scientific Reports*, 2012, **2**, Article number: 792 doi:710.1038/srep00792.
7. J. C. G. Esteves da Silva and H. M. R. Gonçalves, *TrAC Trends in Analytical Chemistry*, 2011, **30**, 1327-1336.
8. S. N. Baker and G. A. Baker, *Angewandte Chemie International Edition*, 2010, **49**, 6726-6744.
9. C. Ding, A. Zhu and Y. Tian, *Acc Chem Res*, 2013, **47**, 20-30.
10. K. E. Sapsford, T. Pons, I. L. Medintz and H. Mattoussi, *Sensors*, 2006, **6**, 925-953.
11. S. M. Borisov, T. Mayr, G. Mistlberger and I. Klimant, in *Advanced Fluorescence Reporters in Chemistry and Biology. II. Molecular Constructions, Polymers and Nanoparticles*, ed. A. P. Demchenko, Springer, Heidelberg2010, vol. **9**, 193-228.
12. J. Hu, L.-s. Li, W. Yang, L. Manna, L.-w. Wang and A. P. Alivisatos, *Science*, 2001, **292**, 2060-2063.
13. A. P. Demchenko, *Methods Enzymol*, 2008, **450**, 59-78.
14. A. P. Demchenko, *Luminescence*, 2002, **17**, 19-42.
15. D. M. Jameson and J. C. Croney, *Comb Chem High Throughput Screen*, 2003, **6**, 167-173.
16. D. M. Jameson and J. A. Ross, *Chemical Reviews*, 2010, **110**, 2685-2708.
17. R. M. Clegg, *Current Opinion in Biotechnology*, 1995, **6**, 103-110.
18. A. P. Demchenko, *Methods and Applications in Fluorescence*, 2013, **1**, 022001.
19. A. P. Demchenko and A. I. Sytnik, *Journal of Physical Chemistry*, 1991, **95**, 10518-10524.
20. J. Jiang, S. Li and H. Cui, *Chemical Communications*, 2012, **77**, 9634-9636.

21. X. Wang, K. Qu, B. Xu, J. Ren and X. Qu, *Journal of Materials Chemistry*, 2011, **21**, 2445-2450.
22. J.-M. Liu, L.-p. Lin, X.-X. Wang, S.-Q. Lin, L.-H. Zhang and Z.-Y. Zheng, *Analyst*, 2012, **137**, 2637-2642.
23. A. N. Fletcher, *Photochemistry and Photobiology*, 1969, **9**, 439-444.
24. M. R. Eftink, *Topics in fluorescence spectroscopy*, 1991, **2**, 53-126.
25. A. Jaiswal, S. S. Ghosh and A. Chattopadhyay, *Chem Commun (Camb)*, 2012, **48**, 407-409.
26. L. Lin, X. X. Wang, S. Q. Lin, L. H. Zhang, C. Q. Lin, Z. M. Li and J. M. Liu, *Spectrochimica Acta Part A: Molecular and Biomolecular Spectroscopy*, 2012, **95**, 555-561.
27. H. Liu, T. Ye and C. Mao, *Angewandte Chemie International Edition*, 2007, **46**, 6473-6475.
28. Y. P. Sun, B. Zhou, Y. Lin, W. Wang, K. A. Fernando, P. Pathak, M. J. Meziani, B. A. Harruff, X. Wang, H. Wang, P. G. Luo, H. Yang, M. E. Kose, B. Chen, L. M. Veca and S. Y. Xie, *J Am Chem Soc*, 2006, **128**, 7756-7757.
29. S. Ray, A. Saha, N. R. Jana and R. Sarkar, *J. Phys. Chem. C*, 2009, **113**, 18546-18551.
30. P.-C. Hsu, Z.-Y. Shih, C.-H. Lee and H.-T. Chang, *Green Chemistry*, 2012, **14**, 917-920.
31. F. D'Souza and O. Ito, *Chemical Society Reviews*, 2012, **41**, 86-96.
32. H. Ramakrishna Matte, K. Subrahmanyam, K. Venkata Rao, S. J. George and C. Rao, *Chemical Physics Letters*, 2011, **506**, 260-264.
33. M. R. Kagan and R. L. McCreery, *Analytical chemistry*, 1994, **66**, 4159-4165.
34. T. Gokus, R. R. Nair, A. Bonetti, M. Bohmler, A. Lombardo, K. S. Novoselov, A. K. Geim, A. C. Ferrari and A. Hartschuh, *ACS Nano*, 2009, **3**, 3963-3968.
35. Y. M. Long, C. H. Zhou, Z. L. Zhang, Z. Q. Tian, L. Bao, Y. Lin and D. W. Pang, *Journal of Materials Chemistry*, 2012, **22**, 5917-5920.
36. G. Marzari, G. M. Morales, M. S. Moreno, D. I. Garcia-Gutierrez and F. Fungo, *Nanoscale*, 2013, **5**, 7977-7983.
37. D. Pan, J. Zhang, Z. Li, C. Wu, X. Yan and M. Wu, *Chem Commun (Camb)*, 2010, **46**, 3681-3683.
38. A. Zhu, Q. Qu, X. Shao, B. Kong and Y. Tian, *Angewandte Chemie*, 2012, **124**, 7297-7301.
39. A. Philippidis, D. Stefanakis, D. Anglos and D. Ghanotakis, *Journal of nanoparticle research*, 2013, **15**, 1-9.
40. Z. Qian, J. Ma, X. Shan, H. Feng, L. Shao and J. Chen, *Chemistry*, 2014, **20**, 2254-2263.
41. L. Tang, R. Ji, X. Cao, J. Lin, H. Jiang, X. Li, K. S. Teng, C. M. Luk, S. Zeng and J. Hao, *ACS Nano*, 2012, **6**, 5102-5110.
42. P. Yu, X. Wen, Y.-R. Toh and J. Tang, *The Journal of Physical Chemistry C*, 2012, **116**, 25552-25557.
43. B. Valeur and M. N. Berberan-Santos, *Molecular Fluorescence. Principles and Applications, 2nd edn.*, Wiley-VCH Weinheim, Germany, 2012.
44. M. Berberan-Santos, E. Bodunov and B. Valeur, *Chemical Physics*, 2005, **315**, 171-182.
45. H. Szmacinski and J. R. Lakowicz, *Sensors and Actuators B: Chemical*, 1995, **29**, 16-24.

46. N. A. Nemkovich, A. N. Rubinov and V. I. Tomin, in *Topics in fluorescence spectroscopy*, ed. J. R. Lakowicz, Plenum Press, New York 1991, vol. **2**, pp. 367-428.
47. P. Anilkumar, X. Wang, L. Cao, S. Sahu, J. H. Liu, P. Wang, K. Korch, K. N. Tackett II, A. Parenzan and Y. P. Sun, *Nanoscale*, 2011, **3**, 2023-2027.
48. X. Wang, K. Qu, B. Xu, J. Ren and X. Qu, *Nano Research*, 2011, **4**, 908-920.
49. A. Bruno, M. Alfe, B. Apicella, C. de Lisio and P. Minutolo, *Optics and lasers in engineering*, 2006, **44**, 732-746.
50. X. Q. Guo, F. N. Castellano, L. Li and J. R. Lakowicz, *Analytical Chemistry*, 1998, **70**, 632-637.
51. N. A. Nemkovich, A. N. Rubinov and V. I. Tomin, *Journal of Luminescence*, 1981, **23**, 349-361.
52. H. Li, X. He, Z. Kang, H. Huang, Y. Liu, J. Liu, S. Lian, C. H. A. Tsang, X. Yang and S. T. Lee, *Angewandte Chemie International Edition*, 2010, **49**, 4430-4434.
53. S. Srivastava and N. S. Gajbhiye, *ChemPhysChem*, 2011, **12**, 2624-2632.
54. X. Wang, L. Cao, S. T. Yang, F. Lu, M. J. Meziani, L. Tian, K. W. Sun, M. A. Bloodgood and Y. P. Sun, *Angew Chem Int Ed Engl*, 2010, **49**, 5310-5314.
55. B. Zhu, S. Sun, Y. Wang, S. Deng, G. Qian, M. Wang and A. Hu, *Journal of Materials Chemistry C*, 2013, **1**, 580-586.
56. G. Eda, Y. Y. Lin, C. Mattevi, H. Yamaguchi, H. A. Chen, I. S. Chen, C. W. Chen and M. Chhowalla, *Adv Mater*, 2010, **22**, 505-509.
57. X. Sun, Z. Liu, K. Welsher, J. T. Robinson, A. Goodwin, S. Zaric and H. Dai, *Nano Research*, 2008, **1**, 203-212.
58. H. Li, Z. Kang, Y. Liu and S. T. Lee, *Journal of Materials Chemistry*, 2012, **22**, 24230-24253.
59. R. G. Mendes, A. Bachmatiuk, B. Büchner, G. Cuniberti and M. H. Rümmeli, *Journal of Materials Chemistry B*, 2013, **1**, 401-428.
60. H. K. Sajja, M. P. East, H. Mao, A. Y. Wang, S. Nie and L. Yang, *Current drug discovery technologies*, 2009, **6**, 43.
61. S. Tan, X. Li, Y. Guo and Z. Zhang, *Nanoscale*, 2013, **5**, 860-872.

Legends to Figures

Fig. 1. Schematic representation of three alternative models of fluorescent C-dots considered in the present study.

Fig. 2. Absorption, excitation and emission spectra of "violet" (a), "blue" (b) and "green" (c) C-dots. Excitation wavelengths: λ_{ex} = 315 and 350 nm (a); 350 nm (b); 425 nm (c). Emission wavelengths λ_{em} = 405 nm (a), 440 nm (b), 530 nm (c).

Fig. 3. Schematic representation of three types of C-dots with different surface groups.

Fig. 4. Fluorescence quenching of "violet" C-dots with iodide ion displayed as Stern-Volmer plots. Measurements were carried out at excitation 350 nm and emission 405 nm.

Fig. 5. Fluorescence decays of "violet" C-dots at different emission wavelengths (λ_{reg} – wavelengths of registration). Excitations are 330 nm (a) and 380 nm (b). IRF – instrument response function.

Fig. 6. Typical anisotropy decays of "violet" C-dots and the influence of viscogen diethylene glycol (DEG). Excitation wavelengths are 330 nm (a) and 380 nm (b).

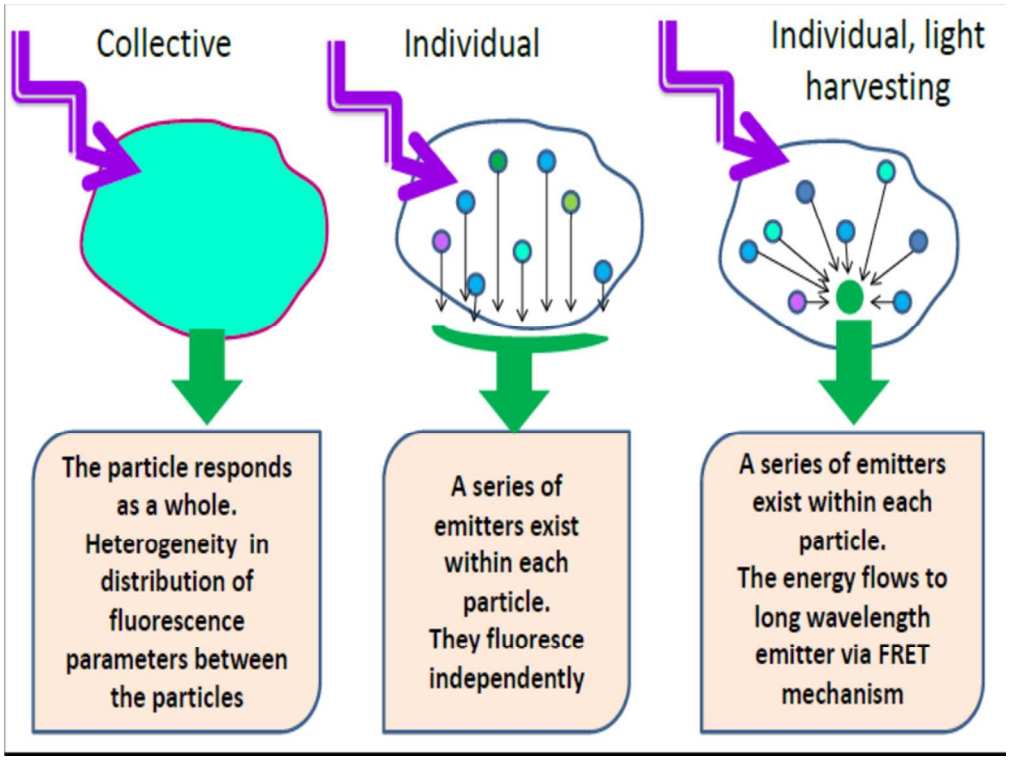

254x190mm (96 x 96 DPI)

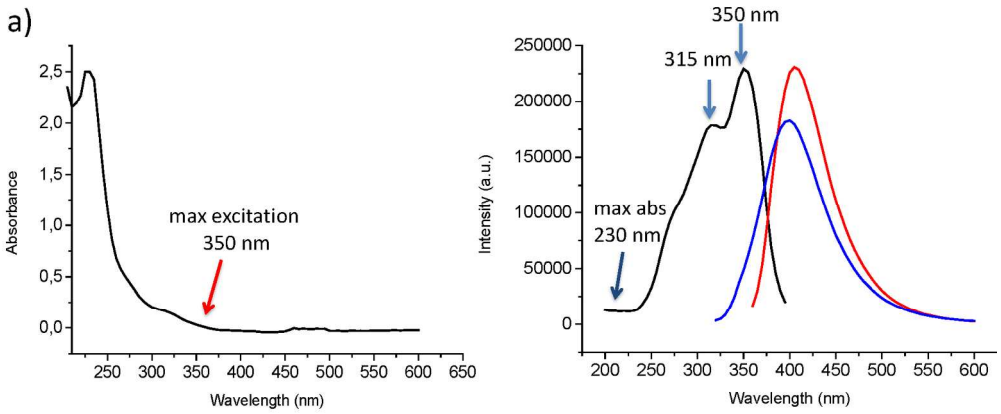

254x105mm (200 x 200 DPI)

b)

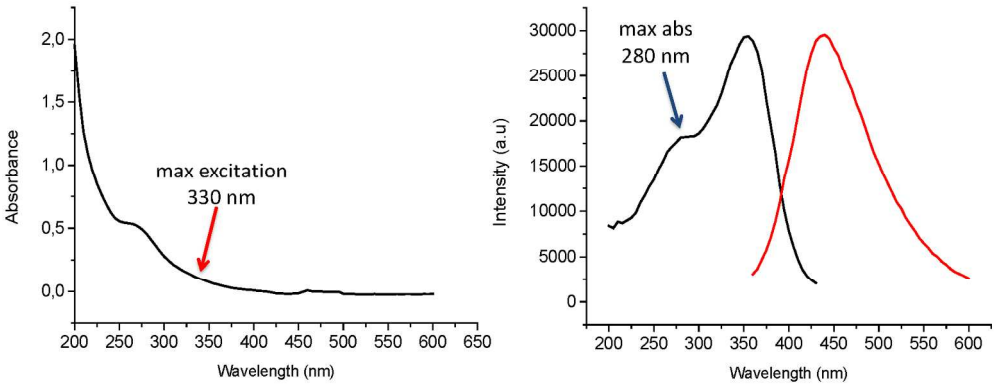

250x105mm (200 x 200 DPI)

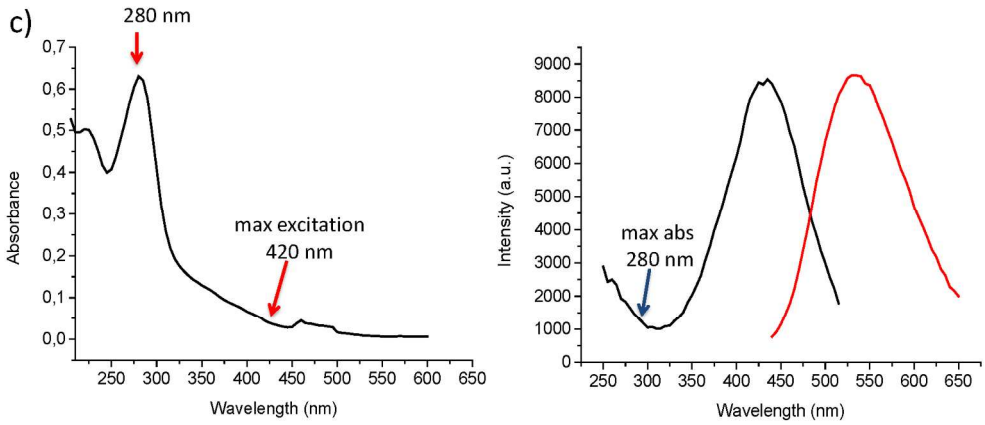

254x108mm (200 x 200 DPI)

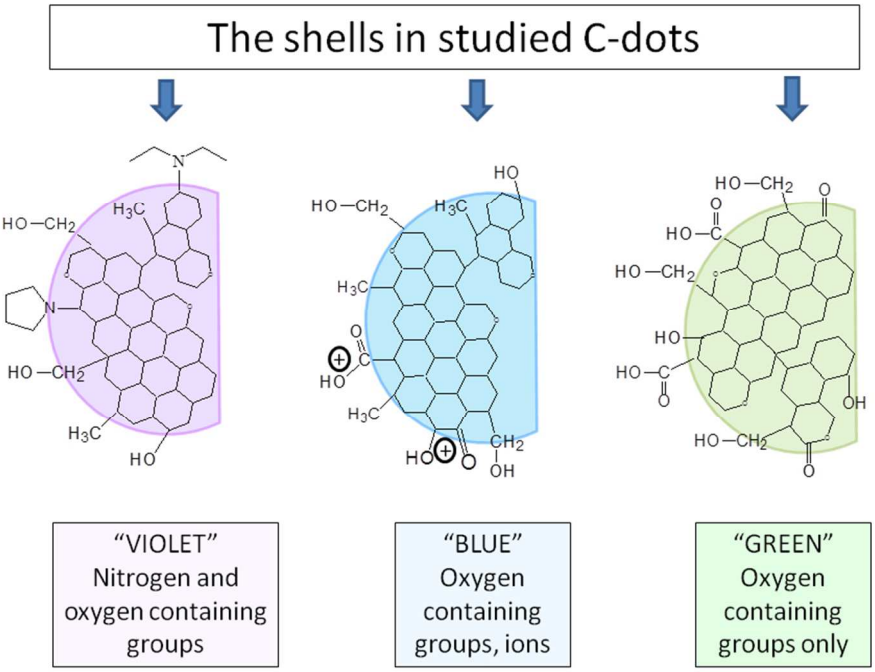

254x190mm (96 x 96 DPI)

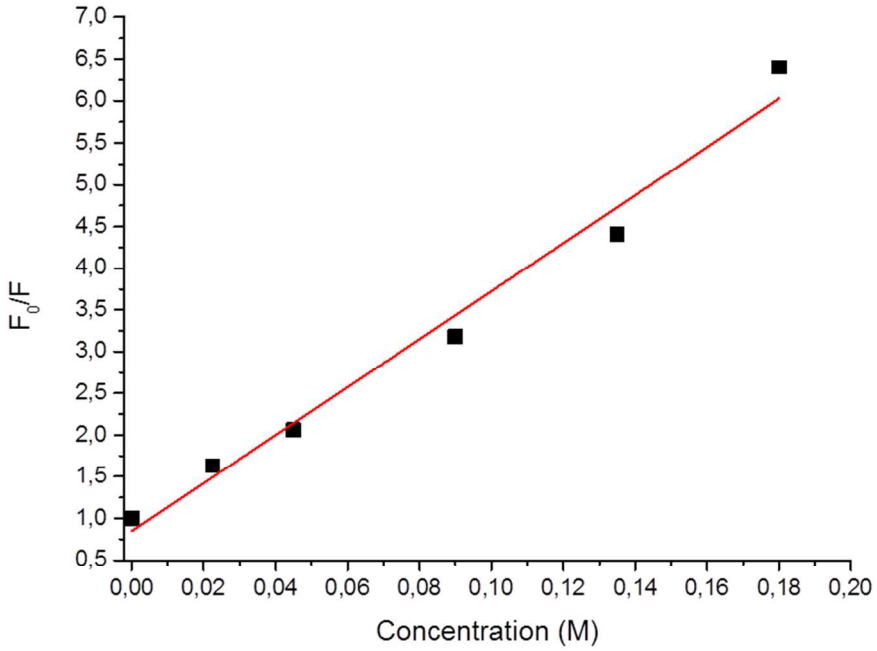

237x164mm (96 x 96 DPI)

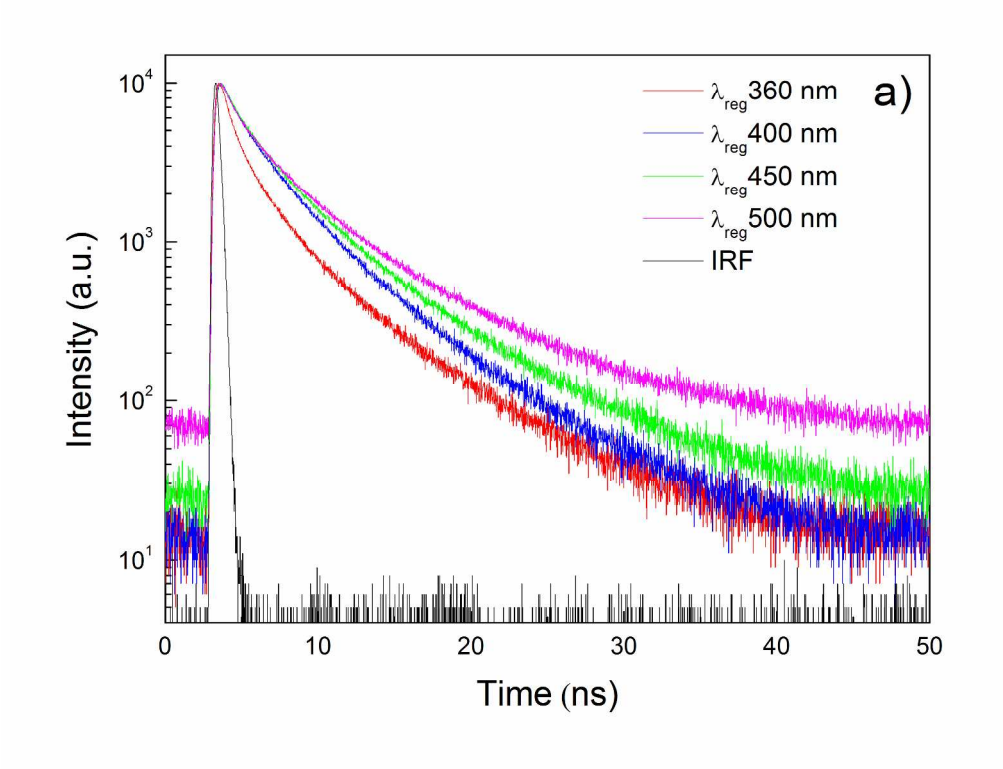

265x205mm (300 x 300 DPI)

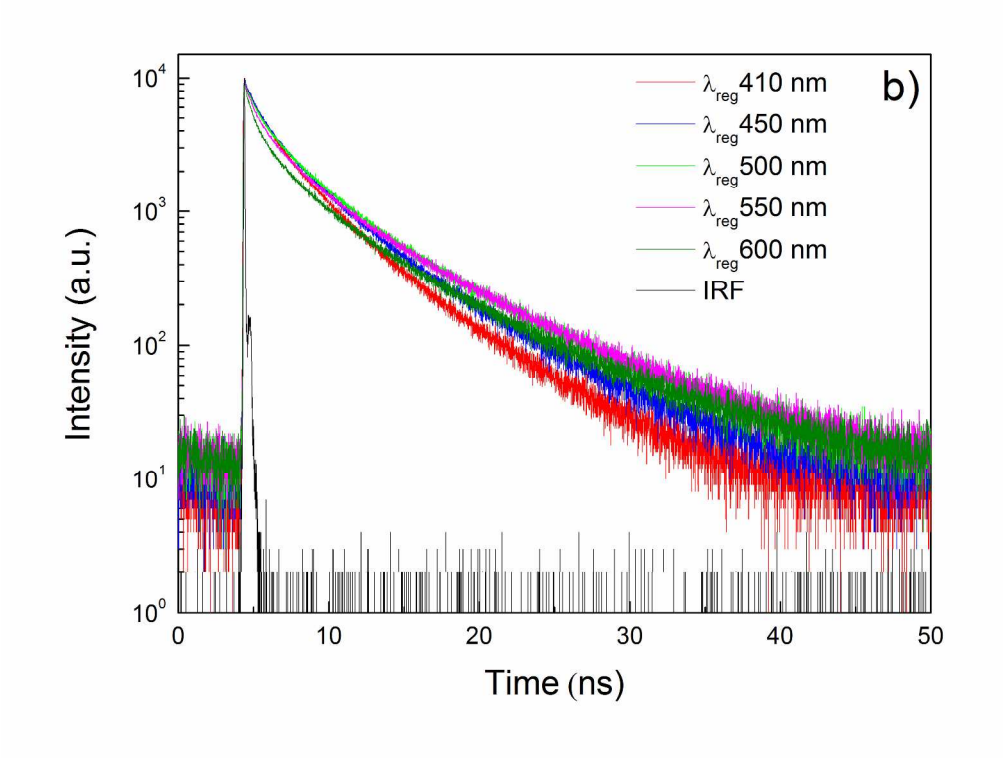

269x205mm (300 x 300 DPI)

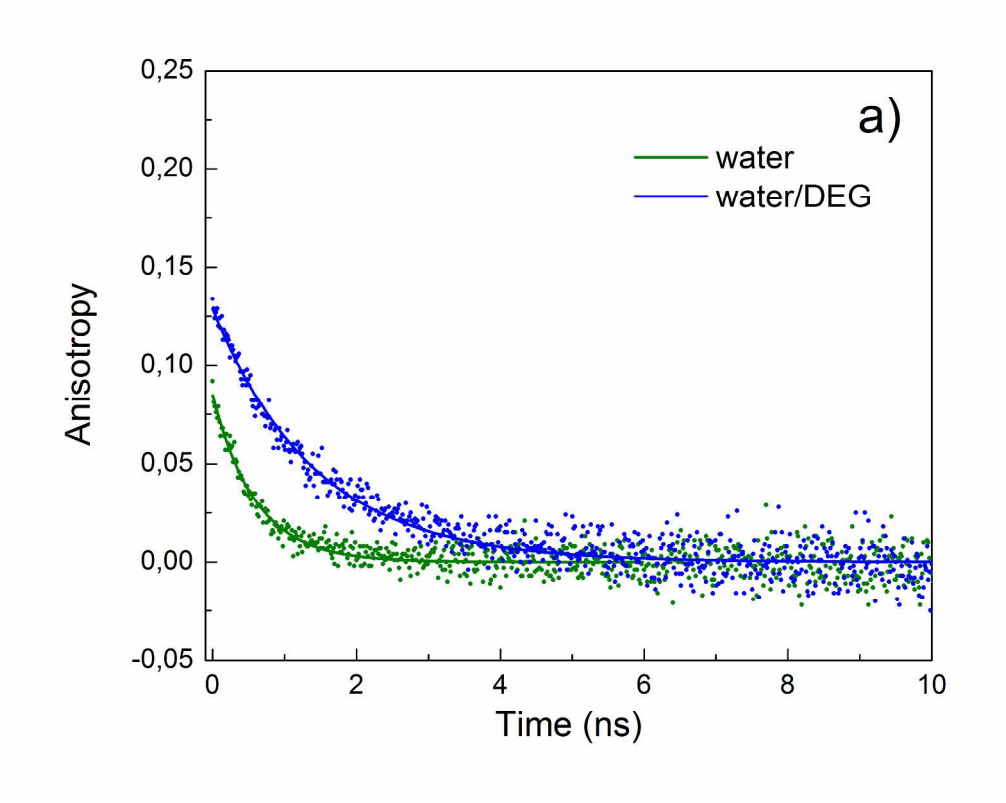

262x210mm (300 x 300 DPI)

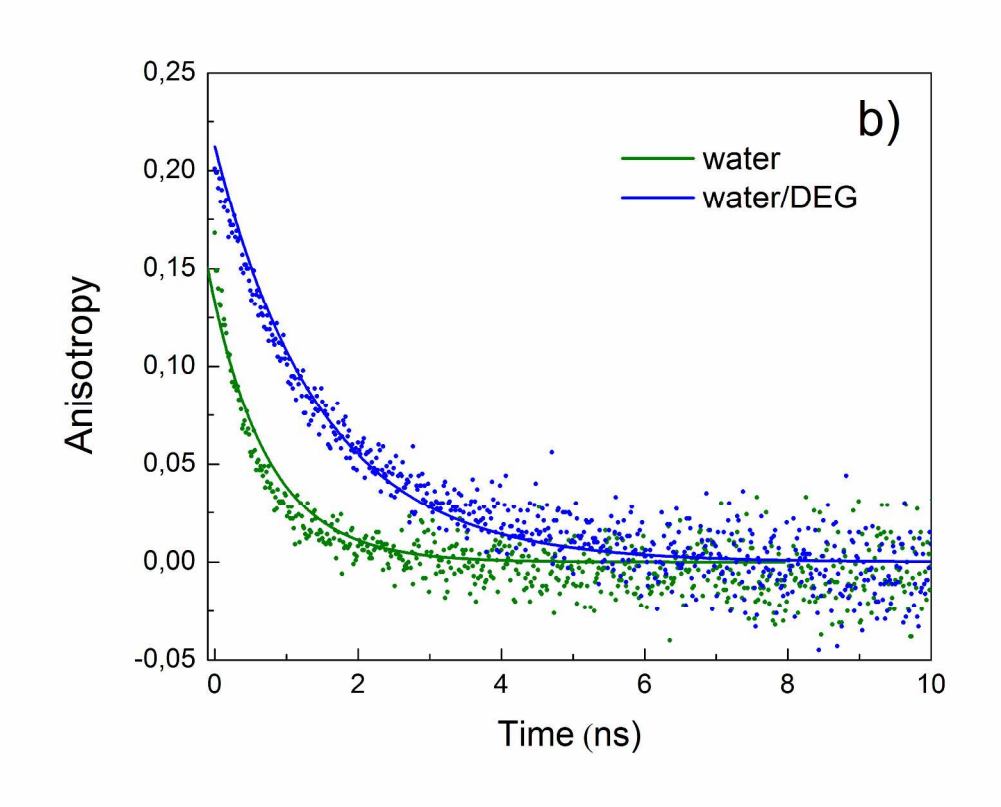

263x213mm (300 x 300 DPI)

Table 1. Summary of major characteristics of studied C-dots. λ_{ex}^{max} and λ_{em}^{max} the positions of excitation and emission band maxima; QY – quantum yield and τ – efficient lifetime of fluorescence. τ_r – rotational correlation time based on anisotropy decay measurements. K_{dyn} is the constant of dynamic fluorescence quenching by iodide.

	"Violet" C-Dots	"Blue" C-Dots	"Green" C-Dots
λ_{ex}^{max}	350	350	425
λ_{em}^{max}	405	440	530
QY	0.28	0.054	0.021
τ (ns)	2.5	2.48	1.98
τ_r (ns)	0.52	0.51	0.80
K_{dyn} ($M^{-1}c^{-1}$)	2.35×10^{10}	1.30×10^{10}	2.24×10^{9}
Size (nm)	5-10	10-50	25-70

Table 2. Analysis of fluorescence emission decays of "violet" C-dots with stretched exponential functions. τ and β are the parameters describing stretched exponential decays.

λ_{exc} = 330 nm, band maximum

Decay parameters	Sample	Emission wavelength			
		360 nm	400 nm	450 nm	500 nm
τ, ns	C-dots	0,565	1,713	1,962	1,943
	C-dots+DEG	0,336	1,221	1,252	0,900
β	C-dots	0,486	0,656	0,650	0,614
	C-dots+DEG	0,443	0,582	0,561	0,491

λ_{exc} = 380 nm, red edge

Decay parameters	Sample	Emission wavelength				
		410 nm	450 nm	500 nm	550 nm	600 nm
τ, ns	C-dots	1,511	1,563	1,484	1,255	0,823
	C-dots+DEG	1,198	1,234	0,962	0,737	0,597
β	C-dots	0,648	0,621	0,577	0,538	0,485
	C-dots+DEG	0,606	0,501	0,522	0,478	0,457

Table 3. Emission wavelength dependence of parameters of anisotropy decay for "violet" C-dots at excitation 330 nm without and with the addition of diethylene glycol (DEG). r_0 is initial anisotropy, τ_r – rotational correlation time and r is the steady-state anisotropy acquired from the decay data.

Anisotropy parameters	Sample	Emission wavelength			
		360 nm	400 nm	450 nm	500 nm
r_0	C-dots	0.125	0.106	0.078	0.074
	C-dots+DEG	0.178	0.153	0.129	0.128
τ_r, ns	C-dots	0.497	0.526	0.606	0.681
	C-dots+DEG	0.953	1.205	1.422	1.515
r, ns	C-dots	0.027	0.017	0.014	0.013
	C-dots+DEG	0.061	0.044	0.039	0.038

Table 4. Emission wavelength dependence of parameters of anisotropy decay for "violet" C-dots at excitation wavelength 380 nm without and with the addition of diethylene glycol (DEG). λ_{exc}=380 nm (at the red edge).

Anisotropy parameters	Sample	Emission wavelength				
		410 nm	450 nm	500 nm	550 nm	600 nm
r_0	C-dots	0.157	0.153	0.147	0.117	0.106
	C-dots+DEG	0.215	0.212	0.198	0.166	0.157
τ_r, ns	C-dots	0.548	0.566	0.584	0.652	0.649
	C-dots+DEG	1.395	1.48	1.578	1.651	1.958
r, ns	C-dots	0.031	0.028	0.026	0.023	0.023
	C-dots+DEG	0.076	0.071	0.067	0.057	0.061

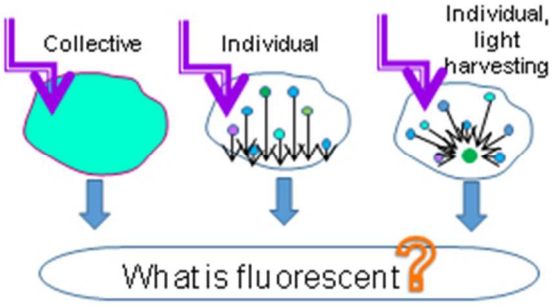

77x43mm (96 x 96 DPI)